Polish J. Chem., **75**, 1–28 (2001) **REVIEW ARTICLE**

Self-Assembling Systems in Restricted Geometry

by A. Ciach and M. Tasinkevych

Institute of Physical Chemistry, Polish Academy of Sciences
Kasprzaka 44/52, 01-224 Warsaw, Poland

(Received June 1st, 2000)

Results obtained within Ciach-Høye-Stell model of oil-water-surfactant mixtures in restricted geometry are reviewed. Special attention is paid to ordering effects of a surface (or two parallel surfaces) close to phase boundaries between lamellar and microemulsion or water-rich phases. Relations between the structure of the confined self-assembling system and the measurable quantities are discussed. Predictions of the Ciach-Høye-Stell model are compared with Landau-Ginzburg and membrane theories and with experimental results.

Key words: surfactant solution, microemulsions, membrane, lattice model, phase transitions, density profile, surface phenomena, confined system, solvation force

1. INTRODUCTION

Surfactant particles can self-assemble into monolayers, when a small amount of them is added to oil-water mixtures. By self-assembly at the oil-water interfaces they prevent unfavorable contacts between the polar and nonpolar components, because one end of surfactant particles is hydrophilic and the other one is hydrophobic. Similar self-assembly into bilayers exhibit surfactant and lipid particles in water or copolymers. Typical size of oil- or water-rich domains, separated by the surfactant monolayer, is 100–1000 Å, whereas the thickness of the monolayer is ~20 Å. One, thus, often models the layers by mathematical surfaces. The oil- or water-rich domains may be closed as in micelles or inverse micelles of various shapes, or not, as for example in multiply connected networks of channels. The domains (and the surfactant surfaces separating them) may form ordered structures, periodic in one, two or three dimensions. As in ordinary crystals, certain elementary cell is infinitely repeated in such ordered phases. The simplest and the most common is a lamellar phase, in which flat oil- and water-rich layers are separated by surfactant sheets. To the most complex structures belong bicontinuous cubic phases [1–4], in which the surfactant is self-assembled into periodic minimal surfaces [5]. When the thermodynamic conditions are suitably changed, the ordered phases can melt. The correlation functions for water (or oil) densities of the resulting microemulsion exhibit damped oscillations. The period of these oscillations is related to the size of the domains of the ordered phases. Hence, on the length scale ~100 Å, the disordered microemulsion resembles locally ordered phases. Simple liquids locally resemble solids in a similar way – the correlation function exhibits damped oscillations with the decay length,

comparable to the period of the structure. When the thermodynamic conditions are changed further (surfactant concentration decreases and/or temperature increases), a disorder line [6–8] is reached. Beyond the disorder line, the correlations of densities decay monotonically on the nanometer length scale. Similar disorder line, but on a molecular length scale, was found in simple liquids [6]. The above observations suggest, that the oil- and water-rich domains play on the nanometer length scale a role analogous to particles in simple fluids on the molecular length scale. However, in various situations the domains behave significantly differently than the particles, especially when the system is under external stress. The domains are compressible and flexible rather than rigid and may change the shape and volume.

2. THEORETICAL APPROACHES

2.1. Membrane Approach: Sufficiently far from the disorder line, when almost all surfactant particles self-assemble into well-defined monolayers, one can develop a statistical-mechanical description, in which the monolayers, rather than particles, play a role of objects. A single monolayer is treated as a nearly incompressible, flexible, elastic membrane. A probability distribution of states of membranes is given by the Boltzmann factor $\sim e^{-\beta \mathcal{F}}$ ($\beta = 1/k_bT$, T is the temperature and k_b is the Boltzmann constant), where the free energy $\mathcal{F}$ is determined by elastic properties of individual membranes and of the whole stack. Due to incompressibility, in-plane deformations of membranes are often neglected. Out of plane deformations change the curvature of the membrane. There are two geometrical invariants of the curvature tensor – the mean, $(c_1 + c_2)/2$, and the Gaussian, c_1c_2, curvatures, where $c_i = 1/R_i$ and R_1,R_2 are principal radii of curvature. The elastic energy of a membrane is approximated by [9–11]

$$\mathcal{F}_{el} = \int dS \left[\sigma + \frac{\kappa}{2}\left(c_1 + c_2 - 2c_0 \right)^2 + \bar{\kappa} c_1 c_2 \right] =$$

$$= \int dS \left[\sigma + \frac{\kappa_+}{2}\left(c_1 + c_2 \right)^2 + \frac{\kappa_-}{2}\left(c_1 - c_2 \right)^2 - 2\kappa c_0 \left(c_1 + c_2 - c_{0)} \right) \right] \qquad (1)$$

where the integral is taken over the area of the membrane, c_0 is the spontaneous curvature related to asymmetry of surfactant particles, σ, κ and $\bar{\kappa}$ are the surface tension, the bending rigidity and the saddle-splay modulus, respectively, and $\kappa_+ = \kappa + \bar{\kappa}/2$, $\kappa_- = -\bar{\kappa}/2$. For incompressible membranes $\sigma = 0$. The shapes and fluctuation spectra of a single membrane are determined by (1).

Undulations of membranes change their effective rigidity – energy cost of bending is different in the presence of ripples – and the elastic properties depend on the length scale. Scale-dependent effective bending rigidity reads [12]

$$\kappa(\xi) = \kappa - \frac{\alpha k_b T}{4\pi}\log(\xi/a) \tag{2}$$

where a is a molecular length and $\alpha = O(1)$ is a constant (in [13] $\alpha = 3$). Similar relations hold for $\kappa_{\pm}$. The length ξ_κ, for which the effective rigidity (2) vanishes, is called the persistence length and reads $\xi_\kappa = a\exp(4\pi\kappa/\alpha k_b T)$ [13]. The persistence length corresponds to the distance up, to which the membrane conserves its orientation (remains flat), *i.e.* to the correlation length for vectors normal to the membrane.

Two nearly flat membranes interact with each other at short distances [14]. Also, the presence of a fluid, confined between them, leads to an additional force, related to excess pressure over the value fixed by the bulk reservoir and called solvation force or disjoining pressure. Thermally excited undulations of membranes (if $\kappa \sim 1 - 10 k_b T$) also contribute to the free energy of a pair of membranes and lead to effective steric repulsions between them [15]. Due to the Gauss-Bonnet theorem, $\int dS c_1 c_2 = 2\pi\chi_E$, the Gaussian-curvature term has no effect, when the topology of the surface does not change. This is because the Euler characteristic χ_E is topological invariant. If $\bar{\kappa}$ is ignored, the free energy functional of a pair of nearly flat membranes can be approximated by the effective Gaussian functional [16]

$$\mathcal{F}[\ell] = \int d^2x\left[\frac{1}{2}\kappa_r(\nabla^2\ell)^2 + \frac{1}{2}\kappa_r\xi_{\|}^{-4}\ell^2\right] \tag{3}$$

where ℓ is a local deviation of a distance between the membranes from the average, $P = \alpha(\beta\kappa_r)^{-1/2}\xi_{\|}$. In the above $\xi_{\|}$ is a correlation length in a direction parallel to the membranes and $\alpha = O(1)$ is a constant. P is proportional to the standard deviation of the membrane position from the average – the separation of membranes is driven by their fluctuations [17]. Terms of higher order in ℓ can be neglected, since their only effect is to renormalize κ into κ_r [16,18].

A whole stack of nearly flat membranes, in which the free-energy of the nearest-neighbors is given by (3), can be described in a continuous approximation by the free-energy $\mathcal{F} = \int \mathrm{d}\mathbf{r} e$ with the free-energy density e, proposed earlier for smectic liquid crystals [19],

$$e = \frac{\bar{B}}{2}(\partial_z u)^2 + \frac{\kappa_r}{2P}(\partial_x^2 u + \partial_y^2 u)^2 \tag{4}$$

$u(x, y, z)$ is a locally varying displacement and describes small deformations of the ideal order and $\bar{B}$ is the compressibility modulus. By comparing (3) and (4) one can relate $\bar{B}$ to κ_r. The relation reads

$$\bar{B} = \alpha^4\frac{(k_b T)^2 P}{\kappa_r(P-\varepsilon)^4} \tag{5}$$

ε denotes the thickness of the monolayer. In the pioneering work of Helfrich [15] $\alpha^4 = 9\pi^2/64$.

When the distance between the membranes grows and becomes comparable to the persistence length ξ_κ, no direction is distinguished and the stack of membranes becomes isotropic as in a random bicontinuous phase. However, the experiments show that the melting of the lamellar phase takes place for significantly smaller distances between the membranes [20,21]. Also, recent measurements [22] show that the experimental points for $\overline{B}$ lie in a region between the theoretical curves (5), corresponding to two significantly different values of κ_b.

Recall that in the above description the effect of $\overline{\kappa}$ is ignored. However, topological fluctuations in a form of passages between neighboring membranes (cylinders connecting "holes" in the two membranes) or in a form of droplets were observed experimentally [20,21,23,24] and in Monte Carlo (MC) simulations [25–27]. Their effect is particularly significant for the melting of the lamellar phase [12,25]. From the second equality in (1) with $\sigma = 0$ and $c_0 = 0$ one sees that for $\kappa_- < 0$ ($\overline{\kappa} > 0$) the lamellar phase is unstable with respect to formation of minimal surfaces (with $c_1 = -c_2$) or for $\kappa_+ < 0$ with respect to formation of droplets (with $c_1 = c_2$) [12]. Melting of the lamellar phase is given by $\kappa_-(\xi) = 0$ [11,28], where the scale-dependent $\kappa_-(\xi)$ is given by an equation analogous to (2). The distance between the layers at this instability is comparable to $\xi_{\overline{\kappa}} = a \exp(4\pi\overline{\kappa}/\alpha_{\overline{\kappa}} k_b T)$. The passages certainly change the elastic properties of the stack of membranes. The dependence of the elastic constant $\overline{B}$ on the saddle-splay modulus $\overline{\kappa}$ has not been determined yet.

2.2. Landau-Ginzburg Approach: The membrane approach is particularly suitable for studying elastic properties of amphiphilic systems. Unfortunately, it is very difficult in the case of bicontinuous structures and in the presence of topological fluctuations. Microemulsions can be more conveniently described within a framework of Landau-Ginzburg theories, in which the state of the system is determined by local concentrations of oil, water, and amphiphiles, $\rho_o(\mathbf{r})$, $\rho_w(\mathbf{r})$, $\rho_{amp}(\mathbf{r},\omega)$, respectively. The fields ρ_i are defined on a mesoscopic length scale. Since one end of the amphiphile attracts oil and the other one attracts water, the interactions with amphiphiles depend on their orientations ω. In more sophisticated descriptions orientational degrees of freedom of polar water particles are also taken into account [29]. Statistical distribution of the states is described by a free-energy functional $\mathcal{F}[\rho_o, \rho_w, \rho_{amp}]$.

In principle, by integrating out the surfactant degrees of freedom, one can obtain a functional depending on a single order-parameter (OP), $\phi = \rho_o - \rho_w$. In practice one assumes that a good approximate form of a functional of ϕ can be obtained on a phenomenological level. The functional is constructed in such a way that one requires agreement between predicted and experimental results for phase equilibria and structures of the uniform phases. One assumes [30]

$$\mathcal{F}[\phi] = \int d\mathbf{r}\left(c(\nabla^2\phi)^2 + g(\phi)(\nabla\phi)^2 + f(\phi) - \mu\phi\right) \tag{6}$$

The function $f(\phi)$ must have three minima for $\phi = \phi_b$, where $\phi_b = \phi_o, \phi_w, \phi_m$, so that the three-phase coexistence between oil ($\phi = \phi_o$), water ($\phi = \phi_w$) and microemulsion ($\phi = \phi_m$) can take place. Typically one assumes that in balanced microemulsions (with $c_0 = 0$) $\phi_m = 0$. The structure factor of uniform phases (Teubner-Strey (TS) form) is

$$S(q) \propto \left(\frac{f''}{2} + gq^2 + cq^4 \right)^{-1} \tag{7}$$

with f'' calculated at ϕ_b and $g = g(\phi_b)$, $\phi_b = \phi_o, \phi_w$ or ϕ_m. $S(q)$ describes structureless oil- and water-rich phases if $g(\phi_{o/w}) > 0$. If $g < 0$, $S(q)$ assumes maximum for $q \neq 0$, as in microemulsions. It is, thus, assumed that $g(\phi_m) < 0$.

In microemulsion the correlation function, $G(r) = \langle \phi(\mathbf{0})\phi(\mathbf{r}) \rangle - \langle \phi(\mathbf{0}) \rangle \langle \phi(\mathbf{r}) \rangle$, in the real-space representation exhibits damped oscillations with a period λ and decay length ξ

$$G(r) \propto \frac{\lambda}{2\pi r} e^{-r/\xi} \sin \frac{2\pi r}{\lambda}; \quad \xi = \left[\frac{1}{2} \left(\frac{f''}{2c} \right)^{1/2} + \frac{1}{4} \frac{g}{c} \right]^{-1/2}; \quad \frac{\lambda}{2\pi} = \left[\frac{1}{2} \left(\frac{f''}{2c} \right)^{1/2} - \frac{1}{4} \frac{g}{c} \right]^{-1/2} \tag{8}$$

The TS form very well agrees with experiments [31,32]. [Actually, a still better fit, particularly for large q, is obtained [33] when (7) is multiplied by $(q^2 + q_p^2)^{-1}$. In [34] q_p is related to the persistence length.] The model (6) predicts stability of the lamellar phase and metastability of numerous bicontinuous cubic phases [2,3,35]. Due to its simplicity, the model is very popular, for reviews see [8,36].

The LG model can be reduced to the membrane description if only a certain class of fields $\phi(\mathbf{r})$ is taken into account. Assume oil-water coexistence and the interface between oil and water located at $z = 0$. The equilibrium OP, $\Phi(z)$, minimizes (6) with appropriate boundary conditions ($\Phi(-\infty) = \phi_o$, $\Phi(\infty) = \phi_w$). If all the fluctuations $\phi(\mathbf{r})$ are neglected, except from capillary waves $\phi(\mathbf{r}) = \Phi(z - u(x,y))$, where $u(x,y)$ describes deviations (small and smooth) of the interface positions from the average $z = 0$, then the functional (6) is reduced to (1) and the parameters σ, κ and $\bar{\kappa}$ describing the surface tension and elastic properties of the interface are expressed as functionals of $\Phi(z)$ [8,25,37].

The level surfaces $\phi = \phi_m$, at which $\phi(\mathbf{r})$ assumes the value corresponding to the bulk microemulsion, are often identified with surfactant monolayers. With this identification the correlations of the surfaces

$$G_{film} \sim \langle \, | \nabla\phi(\mathbf{r})|\delta(\phi(r))|\nabla\phi(\mathbf{0})|\delta(\phi(\mathbf{0})) \rangle \tag{9}$$

where δ is the Dirac δ-function, are identified with the surfactant-surfactant correlation function. Qualitative agreement with experiments for surfactant structure factor

[21] was obtained in (MC) simulations [38]. Note that the surfactant-surfactant correlations can be reduced to correlations of level surfaces only when the surfactant concentration does not fluctuate independently of ϕ, and one can assume that the surfactant degrees of freedom are reduced to oil-water interfaces. [In fact, when all amphiphiles completely saturate oil-water interfaces, the same form of the free energy should result if the amphiphilic degrees of freedom are reduced to interfaces or are integrated out]. The independent fluctuations of the surfactant concentration can be taken into account in a form of a scalar OP, ρ, equal to a deviation of $\int d\omega \rho_{amp}(\mathbf{r},\omega)$ from the average value. Phenomenological functional of ϕ and ρ has been considered in [39]. The structure factor for the surfactant, calculated to 1-loop order, agrees semi-quantitatively with experimental results (for not too large q). In particular, q^{-1} and q^{-2} forms for $q \to 0$ and for large q respectively were found.

In the semi-infinite system the bulk free-energy (6) must be supplemented with the surface term and in slits by two surface terms for two confining surfaces. The surface term describes interactions between the surface and various components of the mixture and the enhancement of the effective interactions in the boundary layer (including missing neighbors). One assumes

$$\mathcal{F}_s = \int_{\partial V} d^{d-1}\mathbf{r}(w_s\phi^2 + \mu_s\phi + g_s(\nabla\phi)^n) \tag{10}$$

Some authors choose $n = 1$ [40,41], others [25,42] assume $n = 2$.

When the surfactant volume fraction is comparable to volume fractions of oil and water and in other cases in which the surfactant degrees of freedom cannot be reduced to local oil-water interfaces, it is advantageous to consider a more general description, like the one presented below.

2.3. Quasi-Microscopic Approach; CHS Model: Self-assembling of surfactant particles, added to a mixture of polar and nonpolar components, follows from their amphiphilic nature – one end of the amphiphile is hydrophilic and the other one is hydrophobic. The same properties of interactions, crucial for self-assembly, are shared by many substances. The generic models with simplified interactions, that capture the features of the interactions which are common for the systems exhibiting self-assembly, should correctly describe their universal properties [8]. One assumes that the universal properties should be described by the generic models in which: (a) similar particles (or particle parts) attract each other and different particles (or particle parts) repulse each other; (b) one end of the amphiphile attracts oil and the other one attracts water. Different models, both in continuum [43–46] and on a lattice [47–56] were introduced and studied. Here, we concentrate on the lattice model introduced by Ciach, Høye and Stell (CHS) [48]. In general, M orientations of amphiphiles, uniformly distributed over a unit sphere, are considered. Every lattice site is occupied by either oil-, water-, or an amphiphile in an orientation $\hat{\omega}_m$, $m = 1, ..., M$, there are thus $2 + M$ microscopic states $\hat{\rho}_i(\mathbf{x})$ at each lattice site $\mathbf{x}$. $\hat{\rho}_i(\mathbf{x}) = 1$ (0) if the site $\mathbf{x}$ is (is not) occupied by the state i, where $i = 1,2, ..., 2 + M$ denotes water, oil and surfactant in dif-

ferent orientations respectively. In the case of close-packing and oil-water symmetry, only one chemical potential variable is relevant, namely $\bar{\mu} = \mu_1 - \mu_{surf} = \mu_2 - \mu_{surf}$, with $\mu_{surf} = \mu_i$ for $i > 2$. The Hamiltonian in the presence of external fields $h_i(\mathbf{x})$ can be written as:

$$H = \frac{1}{2} \sum_{\mathrm{x} \neq \mathrm{x}'} \sum_{i,j} \hat{\rho}_i(\mathbf{x}) \mathrm{U}_{ij}(\mathrm{x} - \mathrm{x}') \hat{\rho}_{\mathrm{j}}(\mathbf{x}') + \sum_{\mathrm{x}} \sum_{i} \mathrm{h}_i(\mathbf{x}) \hat{\rho}_i(\mathbf{x}) - \bar{\mu} \sum_{\mathrm{x}} (\hat{\rho}_1(\mathbf{x}) + \hat{\rho}_2(\mathbf{x})) \quad (11)$$

In the simplest version of the CHS model, a simple cubic lattice with the lattice constant $a \equiv 1$, identified with the length of the surfactant, is considered. Only nearest-neighbors interact and the interaction energy between particles of species i, j at the sites $\mathbf{x}, \mathbf{x}'$ respectively, $\mathrm{U}_{ij}(\mathbf{x} - \mathbf{x}')$, vanishes for $|| \mathbf{x} - \mathbf{x}' || \neq 1$. In the simplest version of the model, the interactions between amphiphiles are neglected. In the case of oil-water symmetry, only two parameters characterize the interactions: b is the strength of the water-water (oil-oil) interaction and c describes the interaction between water (oil) and an amphiphile. The interaction between amphiphiles and ordinary molecules is proportional to a scalar product between the orientation of the amphiphile and the distance between the particles, $\mathbf{x} - \mathbf{x}'$. Expressions for $\mathrm{U}_{ij}(\mathbf{x} - \mathbf{x}')$ are given in [57,58] for various versions of the CHS model. Because the amphiphiles do not interact with each other in the original CHS model, one can exactly integrate their degrees of freedom and obtain an effective Hamiltonian depending only on a difference between oil and water densities. Such a procedure has been performed for the orientations restricted to unit lattice vectors ($M = 2d$) in [59,60]. One should note that the resulting effective Hamiltonian is much more complicated than the continuous phenomenological form (6). In particular, up to 7 lattice-site interactions (central site + $2d$ nearest neighbors) have to be taken into account, whereas in a lattice analog of (6) only up to three lattice site interactions are included.

The model is designed for description of the balanced systems, with $c_0 = 0$. Unless the model is extended to account for asymmetry of interactions, the phase diagram it predicts cannot agree with experimental ones. The discrepancies correspond to stability regions of unbalanced systems ($c_0 \neq 0$) in real substances. For balanced systems, however, many phenomena can be correctly described, despite the fact that some other parts of theoretical and experimental phase diagrams disagree. Extensions of the CHS model are possible if nonsymmetric effective interactions are suitably defined. The interactions between amphiphiles, supporting formations of monolayers, can be taken into account in still another generalization of the CHS model [58]. In contrast to the phenomenological and LG approaches, once the interaction parameters b and c are fixed in the CHS model, there are no other parameters, which could be fitted to the experimental results. The only other parameters in this approach are thermodynamic variables.

It is impossible to solve the CHS model exactly, except for one-dimensional systems [61]. In practice one can obtain approximate results within a mean-field (MF)

theory or by MC simulations. Within the MF approximation the microscopic configurations $\hat{\rho}_i(\mathbf{x})$ occur with a probability proportional to the Boltzmann factor

$$\exp\left(-\beta \sum_{\mathrm{x}} \sum_{i}\left(\phi_i(\mathbf{x})\left(\hat{\rho}_i(\mathbf{x})-\frac{1}{2}\rho_i(\mathbf{x})\right)+h_i(\mathbf{x})\hat{\rho}_i(\mathbf{x})-\bar{\mu}(\delta_{i1}+\delta_{i2})\hat{\rho}_i(\mathbf{x})\right)\right) \tag{12}$$

where $\phi_i(\mathbf{x}) = \sum_{\mathrm{x}'}\sum_{\mathrm{j}} \mathrm{U}_{\mathrm{ij}}(\mathbf{x}-\mathbf{x}')\rho_j(\mathbf{x}')$ is the mean field and $\rho_i(\mathbf{x})$ is the MF-average of $\hat{\rho}_i(\mathbf{x})$, introduced here to compensate the double counting of pairs of sites. The grand thermodynamic potential of the system, confined between two identical surfaces $x_d = 0$ and $x_d = L + 1$, perpendicular to the d-direction in MF takes the form:

$$\Omega(\tau, \mu, L) = \sum_{\mathrm{x}} \sum_{i} \rho_i(\mathbf{x})\left(\tau \ln(\rho_i(\mathbf{x})) + \frac{1}{2}\phi_i(\mathbf{x}) + h_i(\mathbf{x}) - \mu(\delta_{i1}+\delta_{i2})\right) \tag{13}$$

Here, the first summation is taken only over the region $0 < x_d < L + 1$. $\tau = 1/\beta\mathsf{b}$ is the dimensionless temperature, $\mu = \bar{\mu}/\mathsf{b}$, and Ω is also measured in units of b. The distance in (13) is measured in units of the lattice constant, a ~20 Å, comparable to the size of amphiphiles.

The equilibrium bulk densities $\rho_i(\mathbf{x})$ correspond to the global minimum of the thermodynamic potential Ω (13), with $h_i = 0$ and $L \to \infty$. There are many local minima corresponding to various metastable phases with different periods. In practice one can find local minima of Ω by solving a set of self-consistent equations for densities [62]. The stable structure is identified with the one giving the lowest minimum. The self-consistent equations for densities can be solved only numerically and only in finite systems. However, in infinite periodic structures Ω per lattice site, ω_b, is the same as in a finite system with periodic boundary conditions, if the size of the finite system is equal to the period of the infinite periodic structure.

Within MF stability regions of uniform oil-, water-, surfactant-rich (microemulsion) as well as swollen lamellar and bicontinuous ordered phases have been determined [58,62–64]. The transitions between microemulsion and coexisting oil- and water-rich phases or the ordered periodic phases are continuous in the simple MF approximation above a tricritical point. However, these transitions turn to be first order, if the surfactant degrees of freedom are integrated out and only then the MF approximation is applied [59].

Close to continuous transitions the period of the lamellar phase is determined by the period of critical density fluctuations, which is a real number. Hence, in this region lamellar phases with periods incommensurate with the lattice are stable. The stable phase in this case can be found only approximately and the accuracy of the approximation is limited by the size of the finite system with periodic boundary conditions used for calculations. For example, if the period of the stable lamellar phase is

12.5 or 13.5, the size of the finite system, which gives the correct ω_b, should be 25 or 27 respectively and it corresponds to 2 periods of the stable incommensurate phase. By such a method periods which are rational numbers can be obtained. ω_b approaches the value of the stable phase when the period of the metastable structure tends to the equilibrium value. Although the model is defined on a lattice, the period of lamellar phases it predicts can be varied continuously in a region of stability of swollen lamellar phases [62,65].

Finding the effects of a single wall is more difficult. To infer the properties of semiinfinite systems from the results, which can be obtained only for finite systems of size L, one has to choose L sufficiently large, so that the finite size effects are irrelevant. In [66] the excess quantity

$$\Omega_{ex}(\tau, \mu, L) = \frac{1}{A}\Omega(\tau, \mu, L) - L\omega_b(\tau, \mu) \tag{14}$$

where A is the surface area of one wall, is calculated as a function of L for L commensurate with the period of the bulk phase. For sufficiently large $L > L_s(\tau, \mu)$, Ω_{ex} assumes a constant value, indicating that for $L > L_s(\tau, \mu)$ the finite size effects are negligible. The wall in this approach is described by geometrical constraints on the size of the system and by an external field $h_i(\mathbf{x}) = h_i\delta(x_d)$, where $x_d = 0$ describes the position of the confining surface. In a slit the structure can be determined directly by finding the lowest value of Ω for various surface-field strengths.

The density of the surfactant averaged over all microscopic states with the probability (12) turns out to be a smooth function. In particular, in swollen lamellar phases the density of surfactant has a nearly sinusoidal shape [62,66]. It indicates that the microscopic configurations with displaced surfactant monolayers occur with a high probability. Indeed, because of the model interactions, the most probable microscopic states in the CHS model correspond to surfactant monolayers separating oil- from water-rich regions. If we neglect other low-probability states, then the model becomes similar to a discrete version of the membrane model. States with displaced monolayers play in this approach a role analogous to undulations in the membrane approach. The width of the oil-water interface is a measure of the displacements (or undulations) of the surfactant layer. One can reduce the generic microscopic models to the membrane models formally. First, one derives LG models from the microscopic models by a suitable coarse-graining procedure [67]. Then, one can further reduce the problem to the membrane approach by ignoring irrelevant degrees of freedom, in a way described in the previous subsection.

An important feature of the CHS model is that no assumptions concerning the geometry and topology of the surfactant monolayers are necessary. The Boltzmann factor (12) automatically discriminates between the relevant and irrelevant states. In contrast, in the membrane approach one always makes various assumptions about the shapes and topology of the membranes to make any calculations possible. Because of

that, the role of the passage formation in melting of the lamellar phase was overlooked for about a decade.

3. RESTRICTED GEOMETRY

External conditions, such as a planar wall or a confinement, can strongly influence systems exhibiting self-assembly. The tendency for formation of various ordered periodic structures or even the self-assembly can be enhanced or suppresed, depending on the chemical nature, shapes, the structure or the size of boundaries of the system. In the self-assembling systems typical size of the structure λ and correlation length ξ are mesoscopic, 2–3 orders of magnitude larger than in simple fluids. The oil- or water-rich domains play on mesoscale a role analogous to particles of simple fluids on microscale. The ratio between the domain size λ and the diameter of a particle, λ/a, tells how further away from the surface the structure of the self-assembling system is disturbed in comparison to simple fluids. In the amphiphilic systems the effect of the wall extends to much larger distances (2–3 orders of magnitude) and the finite-size effects are relevant for systems, whose sizes would be truly macroscopic for simple fluids.

Effects of boundaries are particularly strong close to phase transitions. In simple fluids wetting phenomena accompanying discontinuous transitions [68–71] and the critical adsorption near continuous transitions were extensively studied [70,72]. The effect of the confinement on simple fluids has also drawn much attention. In particular, the capillary condensation and the corresponding critical point, the solvation force and its connection with the structure of confined fluid were extensively studied for slit-like pores [73–81]. Here, we describe ordering and disordering effects of a single planar wall and of slit-like geometry on self-assembling systems. We pay particular attention to lamellar phases and lamellar-microemulsion or lamellar-water/oil phase boundaries.

In the lamellar phases, the planes describing average positions of surfactant monolayers are parallel to each other. In the swollen phases, the distance between the monolayers is large, up to 1000 Å. The monolayers undulate and near a coexistence with microemulsion numerous passages between the nearest monolayers are formed. In microemulsions the monolayers strongly fluctuate and are interconnected, so that the whole system is isotropic. Intuitively one can expect that a solid external wall or a slit should induce parallel alignment of membranes. As we show later, this is not always the case.

3.1. Semi-Infinite Geometry. 3.1.1. Far from Phase Transitions. In the microemulsion the GS model (6) with the surface term (10) predicts the exponentially decaying lamellar order [41]:

$$\langle\phi(z)\rangle \sim \exp(-z/\xi_s)\sin(2\pi z/\lambda_s + \gamma) \tag{15}$$

Here, the domain size λ_s and the decay length ξ_s of the structure induced by the wall are equal to the bulk parameters λ and ξ. γ is needed to accommodate different surface field strengths w_s, μ_s, g_s [41]. Similar results for the density profiles of the components were obtained in the CHS model [66,82] in the case of hydrophilic walls.

A solid wall should suppress fluctuations of the membranes positions. Indeed, a period of a swollen lamellar phase between hydrophilic walls a distance $L > L_s$ apart (see (14) and the discussion below) is smaller than in the bulk phase in the CHS model [66].

3.1.2. Close to Phase Equilibria. Consider first an attractive wall in contact with a gas phase. If the transition to liquid is approached, then a liquid-like layer is formed near the surface. For temperatures higher than the wetting temperature (located at the bulk phase-coexistence) the thickness of the liquid layer grows as

$$\Gamma \sim -\log|\Delta\mu| \tag{16}$$

where $\Delta\mu$ is the distance from the gas-liquid coexistence. In a slit of width L the thickness of the wetting layer grows when the coexistence with the liquid is approached and becomes

$$\Gamma \sim \log L \tag{17}$$

at the capillary condensation, when the liquid-like phase stabilizes in the whole slit. If the wall is preferentially wet by the gas phase, drying of the wall takes place. The above results hold for any order-disorder transition in uniform systems exposed to a wall and follow from the LG functional of the form

$$F[\eta] = \int \mathrm{d}^{d-1}\mathbf{r}_{||} \int_0^\infty \mathrm{d}z \left(\frac{1}{2}(\nabla\eta)^2 + \mathrm{f}(\eta) + \delta(z)\mathrm{f}_1(\eta) \right) \tag{18}$$

where η is a suitable OP for the corresponding order-disorder transition. The bulk behavior is governed by potential density $\mathrm{f}(\eta)$ and $\mathrm{f}_1(\eta)$ describes the contributions due to the surface:

$$\mathrm{f}(\eta) = -h\eta + \frac{a_2}{2}\eta^2 - \frac{a_n}{n}\eta^n + \frac{a_m}{m}\eta^m; \quad \mathrm{f}_1(\eta) = -h_1\eta + \frac{a_1}{2}\eta^2 \tag{19}$$

Here, a_2, a_n, a_m are positive and for systems which exhibit a bulk tricritical point (n, m) = (4, 6). The coefficient a_2 is temperature dependent, all the other coefficients are constant for the gas-liquid coexistence. a_1 is the surface enhancement and is related to the ratio of the microscopic interactions in the bulk and in the surface, h_1 is the difference between the surface and bulk fields [83]. A crucial quantity for studying the wetting is

$$\Gamma = \int_0^\infty \mathrm{d}z(\eta(z) - \eta(\infty)) \tag{20}$$

Γ is called adsorption or coverage and is proportional to the thickness of the wetting layer. In the context of the liquid-gas coexistence Γ describes the total amount of adsorbed liquid.

It is very difficult to study semi-infinite systems within the membrane approach, especially close to phase transitions. The LG approach is more suitable for this problem. However, any functional, which correctly describes the structure of microemulsion, including the simplest form (6), must have a form essentially different from F given by (18). The latter predicts only stability of homogeneous, structureless phases. Since the LG functionals are essentially different from F given by (18), the results obtained for simple fluids may not apply to systems, exhibiting self-assembly on the nanometer length-scale.

Lamellar–water-/oil-rich phase coexistence. The wetting phenomena close to transitions between water- (or oil-) rich and lamellar phases were studied in [42] in the model defined in (6) and (10) in the MF approximation. A line separating the wet from the non-wet region in the space (w_s, g_s) was found for $\mu_s = 0$. In the balanced systems the concentrations of oil and water are equal in symmetric lamellar phases and $\phi(\mathbf{r})$ integrated over the period of the lamellar phase vanishes. In the oil- or water-rich phases $\phi \neq 0$. Hence, for η identified with ϕ, the adsorption Γ describes the wetting layer of the lamellar phase. The dependence of Γ on the distance from the lamellar - oil-rich phase transition, however, is not described in [42].

Lamellar-microemulsion phase coexistence. As already noted, in balanced systems $\phi(\mathbf{r})$ integrated over the period of the lamellar phase vanishes. Also, in balanced microemulsion $\phi_m = 0$. Therefore, the adsorption Γ defined in (20) vanishes or is very close to zero for $\eta \equiv \phi$, regardless of the thickness of the lamellar layer formed between the wall and the microemulsion. The question arises, whether the general features of the surface phenomena, such as given by (17) and (16) are the same in such complex systems as in simple fluids, or are essentially different. Recall the analogy between the complex system on the mesoscopic length scale and a simple fluid on the atomic length scale, discussed in the Introduction. On the length scale of the size of atoms, the simple fluid exhibits the structure described by the pair-correlation function and only on the larger length scale it is uniform. Similarly, on the length scale of ~ 100 Å the complex system exhibits the structure as described by density distributions and on the length scales larger than the period of density oscillations, it is seen as a uniform fluid. In simple fluids the order parameter is the deviation of the local density from the average value in a region of molecular size. By analogy, the order parameter in a complex system should be identified with a suitable description of the deviations of the density from the average value in a region of a linear size of the period of oscillations. In s-component systems, exhibiting lamellar ordering, the density of each component i of the mixture, $\rho_i(z)$ oscillates around the average value $\overline{\rho}_i = \int_{z'=z}^{z+\lambda} dz' \rho_i(z')$, where z is the direction and λ is the period of the density oscillations.

In [66,82] the OP for one-dimensional structures (lamellar order) and for *s*-component mixtures is defined as

$$\eta(z) = \int_{z'=z}^{z+\lambda} dz' \sqrt{\sum_{i=1}^{s} \left(\rho_i(z') - \overline{\rho}_i\right)^2} \tag{21}$$

In a bulk lamellar phase, the shapes of $\rho_i(z)$ are the same in the whole sample and $\eta(z)$ is a positive constant. By definition, $\eta(z) = 0$ in the uniform phase. Near a continuous transition the OP defined in (21) is proportional to the amplitude of density oscillations, which in turn behaves as $|\Delta\mu|^{1/2}$ in the MF approximation [62], where $\Delta\mu$ is the distance from the transition. Thus, at the continuous transition η vanishes within the MF with the proper critical exponent. We have reduced the degrees of freedom, related to the density profiles, to just one number. This is analogous to reducing the atomic degrees of freedom on the atomic length scale to the local density deviations from the average value. Based on this analogy and following the general arguments of Landau, it is postulated in [82] that in the semiinfinite geometry the functional of η should have the form given by (18) and (19), but with the length unit equal to the period of the density oscillations, rather than to a molecular size. The hypothesis that all degrees of freedom, except for η given by (21), are irrelevant for the general features of the surface phenomena should be verified by explicit calculations in models, which correctly predict the structure of microemulsion and lamellar phases. Unfortunately, in the simplest LG model (6) the microemulsion-lamellar phase transition is continuous in the MF approximation [8] and only MC simulations show that the transition is of first order [38]. It makes the problem difficult and the effect of the wall on microemulsion-lamellar phase coexistence was not studied within the LG approach.

CHS model results. Fortunately, in the CHS model the microemulsion-lamellar phase transition is first order below the tricritical point already in the MF approximation and the predictions of the functional (18) can be explicitly tested for η and Γ defined as discrete versions of Eqs. (21) and (20) respectively. In the semiinfinite system, two orientations of amphiphiles are distinguished: the head or the tail can be oriented towards the wall and $M = 2$ is assumed in [66,82]. A hydrophilic surface is modeled by the surface fields h_i identical to interactions with water molecules, U_{i1}. Also, the one-dimensional description can be applied as in standard wetting theories. The density of surfactant, $\rho_{surf}(z)$ and η, calculated near a hydrophilic wall in microemulsion, close to the transition to the lamellar phase, are shown in Fig. 1. The same quantities are shown in Fig. 2 near a neutral wall ($h_i = -1$) in the lamellar phase, close to the transition to the microemulsion. In the case of the hydrophilic wall, the behavior of the adsorption for the lamellar OP η is shown in Fig. 3. Note the perfect agreement with the predictions (16) and (17) for simple fluids.

The phenomenological parameters in (18) and (19) should be related to measurable quantities and to parameters specifying the material properties of the system. In particular, these phenomenological parameters should be functions of ρ_{surf}, τ and the

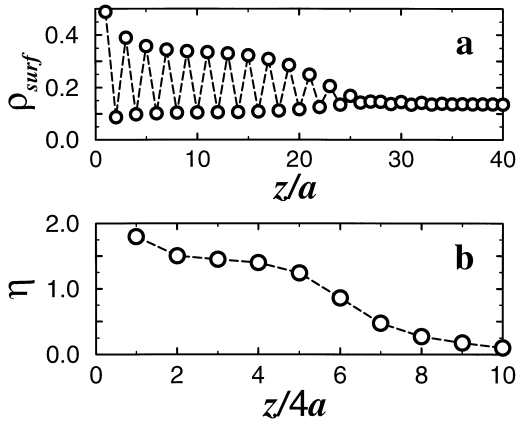

Figure 1. The vicinity of the first-order transition from the microemulsion to the lamellar phase ($\tau = 2.8$, $\mu = 4.3214$, $c/b = 4$, $|\Delta\mu| = 0.0003$) in the one-dimensional system. Walls are covered by a water. **a**: the density of the surfactant as a function of the distance from the wall in units of the lattice constant a. **b**: the lamellar OP η as a function of a distance from the wall measured in units of the period of the lamellar structure equal to $4a$. Dashed lines are to guide the eye.

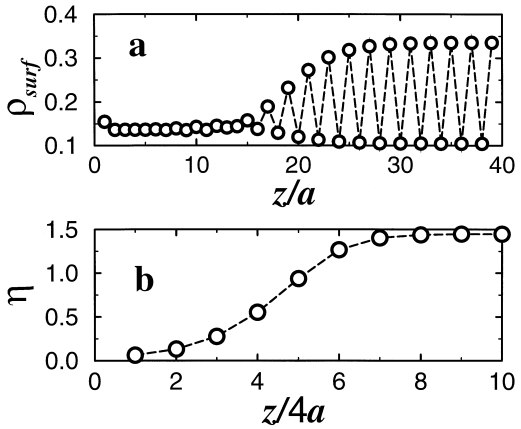

Figure 2. The vicinity of the first-order transition from the lamellar phase to the microemulsion ($\tau = 2.8$, $\mu = 4.3203$, $c/b = 4$, $|\Delta\mu| = 0.0008$) in the one-dimensional system. Walls are not preferential for any state i, *i.e.* $h_i = -1$ for $i = 1,2,3,4$. **a**: the density of the surfactant as a function of a distance from the wall in units of the lattice constant. **b**: the lamellar OP η as a function of a distance from the wall measured in units of the period of the lamellar structure equal to $4a$.

amphiphile strength c if the model (18) is applied for description of wetting in the CHS model. In [66] it is shown that the functional (18) can be derived from the CHS model by a suitable coarse-graining procedure and the explicit expressions for the phenomenological parameters a_2, a_n, a_m in terms of ρ_{surf}, τ and c/b are given there.

The ordering effects of a hydrophobic or a hydrophilic surface in microemulsions and water-surfactant mixtures were studied by neutron reflectometry in [41,84,85] and [86] respectively. When several water-rich layers, separated by surfactant (or

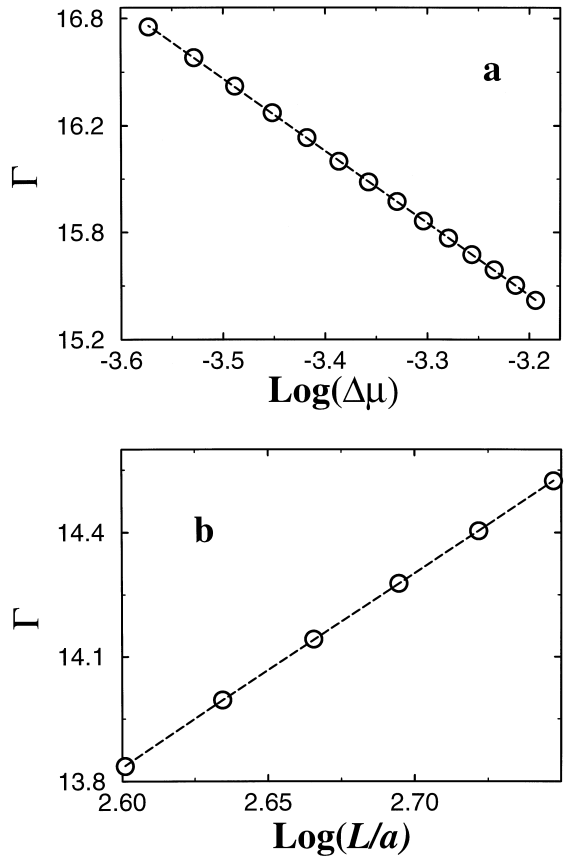

Figure 3. Excess lamellar OP, Γ defined in (20), calculated for one-dimensional system in the case of water-covered walls, for $\tau = 2.8$, $c/b = 4$. **a**: as a function of $\log(\Delta\mu)$, $\Delta\mu$ is the difference between μ and its value at the bulk phase transition. **b**: as a function of $\log(L)$ at the transitions corresponding to capillary condensations. L is the distance between the walls measured in units of lattice constant a. Dashed lines are linear fits.

surfactant-oil-surfactant) layers are formed near the surface, multiple scattering takes place. Experimental reflectivity $R(q)$ depends on the width of the layers and on the water concentrations in them and is related to the near-surface structure in a complicated way. The authors tried to fit their experimental data to the form (15). However, reflectivity $R(q)$ calculated for the structure (15) is essentially lower than the measured values. To fit the data, the authors had to use λ_s significantly smaller than λ and ξ_s significantly larger than ξ. Moreover, the difference between the surface and the bulk parameters increases when the coexistence with the lamellar phase is approached. Such behavior is consistent with the increase of the thickness of the lamellar-like surface layer, predicted by the wetting theory described above.

3.2. Slit Geometry: In order to keep the confining walls at a given distance L, an external force must be applied. For fluids confined between two parallel walls this

force, per unit area of the confining wall, is called solvation force or disjoining pressure [87], f, and can be expressed as an excess pressure over the bulk value p [76]:

$$\mathsf{f} = -\frac{1}{A}\left(\frac{\partial\Omega}{\partial L}\right)_{\mu,T,A} - p \tag{22}$$

Ω is the grand thermodynamic potential and A is the surface area of one wall ($A >> L^2$). For simple fluids the solvation force measured in surface force apparatus experiments [88] shows an oscillatory behavior for separations up to several diameters of fluid particles [89] and with the periodicity approximately equal to one fluid molecular diameter. Oscillatory f results from the packing effects, which also give rise to highly structured density profile $\rho(z)$. All structural deformations and/or transitions, occurring in confined systems (capillary condensation, layering), are reflected in the behavior of the solvation force. Hence, the surface force apparatus measurements provide experimental information about the structure and transitions in the confined systems.

Let us start the description of amphiphilic systems in slits with simple general considerations. Recall the analogy between particles on the molecular length scale and the oil- or water-rich domains on the nanometer length scale. Based on this analogy, one can expect an oscillatory solvation force in microemulsions and lamellar phases, resulting from packing effects of domains. Period of the solvation force should be comparable to the period of the structure λ. Note, however, that the space between particles in simple fluids is empty. In the amphiphilic systems the oil- and water-rich domains are separated by the surfactant monolayers. The monolayers fluctuate and the undulations lead to the formation of a thick interface between the "core parts" of the water- and the oil-rich domains. The width of the interface is determined by the standard deviation from the average of the position of the monolayer. In contrast to simple fluids, the regions between the cores of the oil- and the water-rich domains are thus not empty. Compression or decompression leads to a decreased or increased distance between the core parts of domains respectively. This in turn corresponds to suppression or enhancement of the undulations of the monolayers. Let us fix our attention on lamellar phases of period λ between parallel hydrophilic walls. The equilibrium width L is equal to $L_N = N\lambda + \lambda/2$, where N is integer. By analogy with simple fluids, we may expect that when the equilibrium distance between confining walls L_N is changed to $L + l$ with $|l| > \lambda/2$, then a new lamellar layer is introduced if $l > 0$ or one layer is removed if $l < 0$. At these transitions the solvation force changes discontinuously, due to the abrupt change between the stretched and shrunk structures. Let us assume that the period of the confined lamellar phase is the same in the whole slit. When the equilibrium wall separation L_N is changed to $L_N - \lambda/2$, then $N \to N - 1$ and $\lambda \to \lambda + \Delta\lambda$, with $\Delta\lambda = \lambda/(2N - 1)$. $\Delta\lambda/\lambda$ describes the deformation of the structure, if λ and $\Delta\lambda$ are independent of the distance from the confining walls. At the same time, $\Delta\lambda/\lambda$ describes the enhancement of undulations of the monolayers. There are

two interfaces per one period of the lamellar phase apart from the oil- and the water-rich domains. If we assume that the width of the interface is $W \leq \lambda/4$ and the deformation is uniform, so that the increase of the width is $\Delta W = \Delta\lambda/4$, we obtain the enhancement of undulations $\Delta W/W \geq \Delta\lambda/\lambda$. For large N the enhancement (or suppression) of undulations is small and the confined self-assembling system on the length scale of λ may indeed behave as a simple fluid on the molecular length scale. However, for $N \leq 5$, $\Delta\lambda/\lambda > 10\%$, and the undulations must be strongly enhanced, if one period of the lamellar phase is removed under compression and the structure of the stretched system is the same in the whole slit. On the other hand, the external wall suppresses fluctuations of the monolayers in the near-surface region. One may expect, in agreement with experiments [90], that the suppression of undulations extends to distances $\sim 2\lambda - 4\lambda$ from the wall. For $N \leq 5$ the distance from one or the other wall is $< 3\lambda$ and the undulations should be suppressed rather than enhanced in the whole slit. Results obtained in the semiinfinite geometry show that hydrophilic walls support the formation of lamellar structures with the period equal or lower than in the bulk phases in the near-surface region. Thus, one can expect that the central region of the slit should be deformed. The structure of the central region of the slit should depend on the thermodynamic state of the system, especially on the distance from phase transitions. Consider two interesting examples – neighborhood of the lamellar-microemulsion or the lamellar-oil/water-rich phase transitions. The excess thermodynamic potential in the case of the deformation of the lamellar phase can be approximated by $\Omega_{ex} \approx L\Delta\omega_\ell + 2\sigma_w$, where $\Delta\omega_\ell$ is the increase of the thermodynamic potential density, due to the deformation of the structure and σ_w is the wall-fluid surface tension. Introducing a slab of the uniform phase of width l into the center of the slit and letting the lamellar phase near the surfaces to assume the most favorable period, leads to the excess thermodynamic potential $\Omega_{ex} \approx L\Delta\omega_u + 2\sigma_w + 2\sigma_{u\ell}$, where $\Delta\omega_u$ is the difference between the thermodynamic potential density in the uniform and the stable lamellar phases and $\sigma_{u\ell}$ is the surface tension between these phases. The thermodynamic potential densities of the two phases are only slightly different close to phase coexistence. If also at the coexistence the surface tension between the two phases is low, such that $\Delta\omega_\ell > \Delta\omega_u \ell/L + \sigma_{u\ell}/L$, it should be favorable to form a slab of the uniform phase in the center of the slit, instead of forming the lamellar phase with strong enhancement of undulations. Increasing or decreasing the width of the uniform slab leads to no stress and the period of the near-surface lamellar films can be adjusted with no constrains. The compression should thus lead to a decreased width, $l - \Delta l$, of the uniform layer, with the surface lamellar films unaffected. A rough estimate for the solvation force is $\sim \Delta\omega_u$. Close to phase coexistence, the difference between the bulk thermodynamical potential densities $\Delta\omega_u \to 0$ and the solvation force should be very weak if a uniform layer stabilizes in the center of the slit.

Consider the neighborhood of the lamellar-microemulsion phase coexistence. The mechanism of stabilizing the microemulsion would be to allow for large fluctuations of the monolayers, such that their average positions are no longer fixed in the central layer of width $\approx n\lambda + \lambda/2$, $n \geq 1$. In microemulsion the surfactant volume frac-

tion is lower than in the lamellar phase and the average distance between the monolayers is larger. By forming the slab of microemulsion in the center, the system can adjust to the width of the slit without deforming the near-surface lamellar films. In the case of the lamellar - oil/water-rich phase coexistence, the simplest way of creating a uniform film in the center of the slit would be to remove surfactant-oil-surfactant (for N even) or surfactant-water-surfactant (for N odd) layer from the center of the slit. Then, the two water- or oil- rich layers merge into one, twice as thick, in the center of the slit.

To summarize, for large slits we expect that on the nanometer length scale the confined amphiphilic systems should behave in a way similar to simple fluids on the molecular length scale. For narrow slits, however, substantial difference between the self-assembling systems and the simple fluids should be expected. Unlike particles, the domains can change shape and volume, can merge or be split and the deformed structures should be stabilized in the central region of the slit. The considerations based on general grounds should be verified by explicit calculations. We present the results obtained in the three major approaches below.

3.2.1. Confined Stack of Membranes. Mechanical properties (*i.e.* solvation force for example) of confined lamellar and induced lamellar phases can be conveniently described within the membrane approach. A slab of a lamellar phase should respond elastically to compression or decompression with respect to its equilibrium width L_N. The compressibility modulus of such a slab is given by (5) in the simplest approximation, in which the only fluctuations of the membranes are their undulations. In fact, droplets or passages between the membranes are rare far from the melting point of the lamellar phase and (5) should be a good approximation there. The closer to the melting of the lamellar phase, the more passages are formed and the poorer should be the approximation (5), in which passages are not taken into account. The behavior corresponding to a chain of identical joined springs, each spring representing one lamellar layer, was confirmed experimentally [22,91,92]. While some measurements [93–95] confirmed the form (5), another [22] show that $\overline{B}(P)$, where $P = \lambda/2$, lies between two lines corresponding to two significantly different values of bending rigidity κ. This suggests that in this second case deformations of the perfect lamellar order other than undulations, probably passages, are relevant and change the dependence $\overline{B}(P)$. The agreement between the membrane description and experiments was observed only for large systems, $L > 4\lambda$. For $L < 4\lambda$ substantial deviations from the elastic behavior were observed in agreement with our expectations obtained on general grounds.

3.2.2. Confined Microemulsions and Lamellar Phases in the Landau-Ginzburg Model. Thermodynamic properties, such as analogs of capillary condensations, are not easily described within the membrane approach. It is much easier to study phase transitions in confined self-assembling systems within the LG or CHS models. The LG model (6) with the surface term (10) corresponding to confining walls was applied for studying confined microemulsions in [40] and confined lamellar phases in [25,96,97]. In [40] $g_s = 0$ and $n = 1$ were assumed, whereas in

[25] $n = 2$. Piecewise parabolic f and piecewise constant g allow for analytical results and such forms of these functions were assumed in [40,25]. It was found that the effect of confinement on weakly and strongly structured microemulsions is qualitatively different in this model. In weakly structured microemulsions, with the oil- and water-rich domains of size λ correlated over a short distance ξ, $2\pi\xi/\lambda < \sqrt{3}$, the capillary condensation of a lamellar phase takes place only for narrow slits. In contrast, for $2\pi\xi/\lambda > \sqrt{3}$, lamellar phase stabilizes in slits of arbitrary width. In lamellar [25] and induced lamellar [40] phases expansion of the slit leads to insertions of new layers, accompanied by an abrupt change of the solvation force from the attractive to the repulsive one. In a stretched system, the surface tension of oil-water interfaces becomes negative, signaling the tendency of the system for increasing the surface area, which takes place when a new layer is introduced into the slit [25] and the surface tension changes its sign.

Predictions of the LG model (6), (10) are qualitatively correct. However, it is not clear from the results of [40,25] whether the response of the confined system to compression or decompression is elastic and how it depends on elastic properties of a single membrane and on the period of the lamellar phase. Hence, it is not clear whether the predictions of the LG models for self-assembling confined systems are consistent with the results of the membrane approach and with experiments.

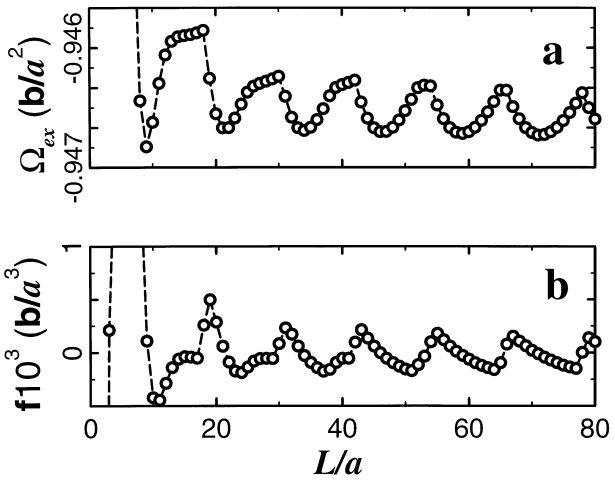

Figure 4. **a**: The excess thermodynamic potential Ω_{ex} (in units of b/a^2), defined in (14), as a function of the wall separation measured in units of the lattice constant a. **b**: The solvation force f (in units of b/a^3) as a function of the wall separation. The thermodynamic variables τ, μ and the material constant c/b of the one-dimensional system correspond to stability of the swollen lamellar phase with $\lambda = 13a$ ($\tau = 0.84$, $\mu = 0.774$, $\mathsf{c}/\mathsf{b} = 1$); the distance from the first-order transition between the water-rich and the lamellar phases is $|\Delta\mu| = 0.003$. Walls are covered by water. Dashed lines are to guide the eye.

The structure of lamellar phases, confined between hydrophilic walls, was studied in MC simulations for the LG model (6) for very narrow slits ($L \leq 2\lambda$) in [96,97]. For such L experiments show deviations from the elastic behavior predicted by the membrane-theories. It turns out that for $L \leq 2\lambda$ the structure significantly differs from shrunk or stretched lamellar phases if L does not match the equilibrium size of the slab. Apart from one (for small L) or two (for larger L) pairs of surfactant monolayers located near the walls, a thick layer resembling microemulsion is formed in the middle of the slit. For nearly neutral walls, simulations suggest the formation of lamellar structures perpendicular to the walls.

3.2.3. Confined Lamellar and Uniform Phases in the CHS Model. Confined lamellar and water-rich phases, in the case of hydrophilic walls, are studied in [65] in one- and three-dimensional versions of the CHS model. In the three-dimensional case the surfactant-surfactant interactions between nearest-neighbors, supporting formations of monolayers, are included. As in [58] two parallel (antiparallel) amphiphiles contribute $-g(+g)$ to the energy of the system if the distance between them is perpendicular to their orientation. In such extended CHS model, the lamellar phases (including the swollen ones) occupy a large part of the phase space. Because the walls break the symmetry, as in the semiinfinite case, we assume that all quantities depend only on the distance from the left wall, z. In the one-dimensional case, the mean-field reads $\phi_i(z) = \sum_{z'=1}^{L} \sum_j U_{ij}(z - z')\rho_j(z')$ (see section 2.3). In the three-dimensional case a term describing the in-plane energy contribution should be added to $\phi_i(z)$.

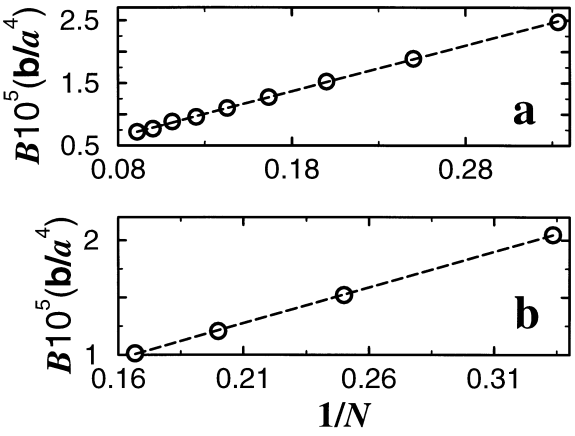

Figure 5. One-dimensional system. The subsequent minima of Ω_{ex} are fitted by quadratic curves $B(L - L_N)^2$, where L_N is the equilibrium separation for N adsorbed layers and B is the coefficient in the fitting curve to the N-th minimum. **a**: B (in units of b/a^4) as a function of the inverse number of adsorbed layers $1/N$. The thermodynamic variables τ, μ and the material constant c/b are the same as in Fig. 4. **b**: B (in units of b/a^4) obtained for the induced lamellar phases as a function of the inverse number of adsorbed layers $1/N$. The parameters τ, μ and c/b correspond to stability of the water-rich phase ($\tau = 0.84$, $\mu = 0.778$, $\mathsf{c}/\mathsf{b} = 1$). The distance from the first-order transition to the swollen lamellar phase is $|\Delta\mu| = 0.001$. Dashed lines are linear fits.

For studying structural deformations in confined system, the crucial quantity is the excess thermodynamical potential Ω_{ex} defined in (14). Ω_{ex} is the effective interaction energy per unit area between the walls plus a term independent of L and related to the total wall-fluid interfacial tension. Then $-\partial\Omega_{ex}/\partial L$ is the solvation force, needed to held the walls at the separation L. The one- and three-dimensional models give qualitatively the same results for lamellar phases of similar periods, thus we present here mainly the results of the simpler, one-dimensional case.

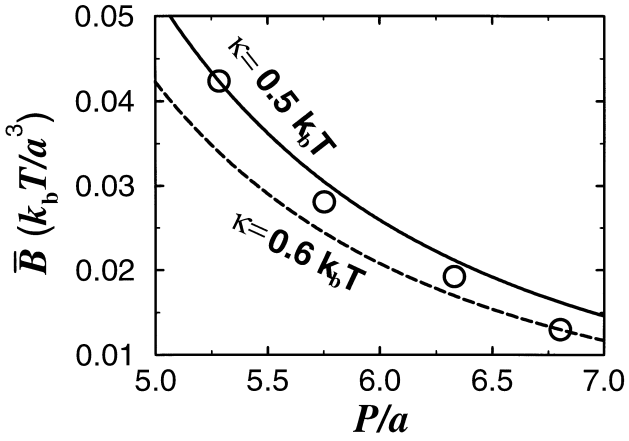

Figure 6. Compressibility modulus $\overline{B}$ (in units of k_bT/a^3) of the swollen lamellar phases as a function of the average distance between the surfactant monolayers, $P = \lambda/2$ (in units of a) in the three-dimensional system. The behavior expected from the phenomenological prediction of Helfrich ((5)) is shown for two values of κ: $0.5k_bT$ (solid line), $0.6k_bT$ (dashed line).

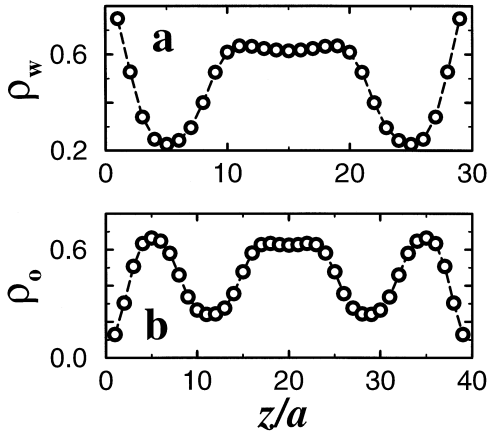

Figure 7. One-dimensional system in the case of intermediate wall separations, $18 < L < 54$. Length is measured in units of the lattice constant a. The thermodynamic variables τ, μ and the material constant c/b are the same as in Fig. 4, period of the bulk lamellar phase is $\lambda = 13$. Walls are covered by water. **a**: the density distribution of water between the walls for the separation $L = 29$. **b**: the density distribution of oil between the walls for the separation $L = 39$.

Swollen lamellar phases. For c/b = 1 the swollen lamellar phases are stable, close to coexistence with the uniform water-/oil-rich phases (water-oil symmetry was assumed). Surfactant concentration at the coexistence is low, $\rho_{surf} \sim 0.12$. The behavior of Ω_{ex} and f, as well as the structure of the confined system, agree with the predictions based on general grounds discussed above. The excess thermodynamic potential per unit area Ω_{ex} and the solvation force f obtained for $\lambda = 13$ in [65] are shown in Fig. 4.

For large separations between surfaces ($N > 4$), the second derivative of Ω_{ex} with respect to L calculated at $L = L_N$, $B = \Omega''_{ex}(L_N)$, is well approximated by a straight line $B = (\overline{B}/2\lambda)N^{-1}$ as a function of $1/N$ (see Fig. 5a). Hence, the response of the system to compression or decompression is elastic, and analogous to the behavior of a series of identical joined springs.

The modulus of compressibility $\overline{B}$ as a function of $P = \lambda/2$ for a three-dimensional system is shown in Fig. 6 (open circles) together with the phenomenological curves (5) for two values of κ, between which the results are located [65]. The discrepancy between the results of the CHS and the membrane models results probably from deformations, such as passages or droplets, neglected in the latter case. For the surface separations, for which the number of adsorbed layers is $N \leq 3$, the stretch strain of layers releases by formation of the uniform water-rich film for $N = 1,3$ (see Fig. 7a), and oil-rich film for $N = 2$ (see Fig. 7b) in the middle of the slit. This agrees with the predictions described above. The formation of the uniform films inside the slit is reflected in the saturated-like behavior of Ω_{ex} and considerably low f for the corresponding surface separations. The elastic behavior of the confined lamellar

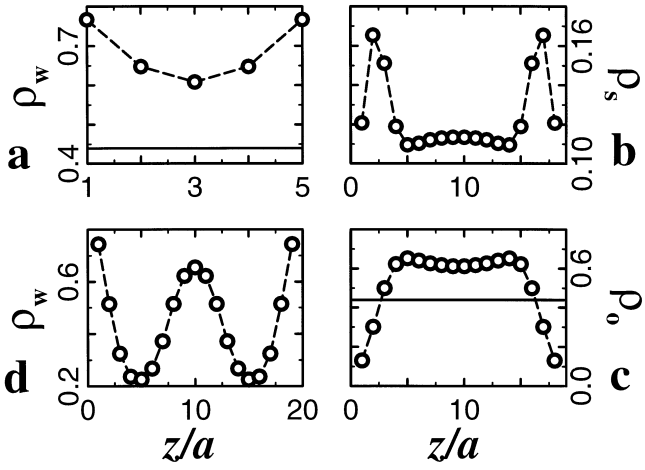

Figure 8. One-dimensional system in the case of small wall separations, $L < 19$. Length is measured in units of the lattice constant a. The thermodynamic variables τ, μ and the material constant c/b are the same as in Fig. 4, and $\lambda = 13$. Walls are covered by water. **a**: the density distribution of water for the separation $L = 5$. The solid line is the average water density in the bulk lamellar phase for the same values of τ, μ, c/b. **b**: the density distribution of the surfactant for the separation $L = 18$. Note the surfactant-rich surface films. **c**: the density distribution of oil for $L = 18$. The solid line is the oil density in the bulk lamellar phase for the same conditions. **d**: the density of water for the wall separation $L = 19$. Dashed lines are to guide the eye.

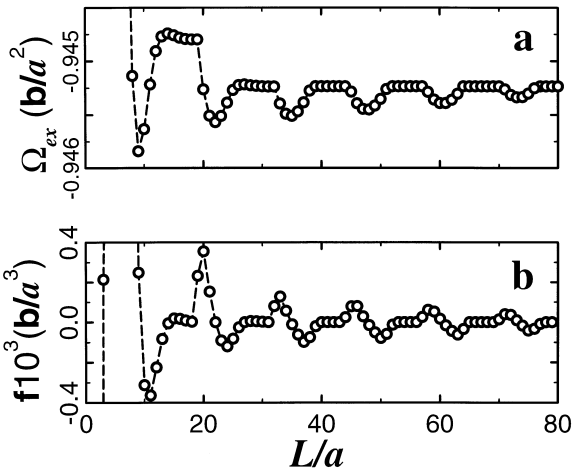

Figure 9. a: The excess thermodynamic potential Ω_{ex} (in units of b/a^2) as a function of the wall separation measured in unit of the lattice constant a. **b**: The solvation force f (in units of b/a^3) as a function of the wall separation. The thermodynamic variables τ, μ and the material constant c/b of the one-dimensional system correspond to the stability of the water-rich phase, close to the coexistence with the swollen lamellar phase ($\tau = 0.84$, $\mu = 0.778$, $c/b = 1$, $|\Delta\mu| = 0.001$). Walls are covered by water.

phase can still be observed, but only for small deviations from the equilibrium separations. The structure for $N < 1$ is shown in Fig. 8.

Water-rich phase. Ω_{ex} and f calculated as functions of the wall separation are shown in Fig. 9. In general, the structure in the slit is determined by the thermodynamical potential density ω_b of the bulk metastable phases. If L matches the period of the metastable phases with low ω_b, the lamellar phase is formed between the surfaces, see Fig. 10a. Otherwise, the water rich phase is formed inside the slit as shown in Fig. 10b, and the solvation force vanishes. The induced lamellar phases also show the elastic response to the confinement, see Fig. 5b, but only for small deviations from equilibrium separations.

Shrunk lamellar phase. Close to the coexistence between the microemulsion and the shrunk lamellar phases, only one metastable phase occurs apart from the other, stable one. This gives qualitatively a different energy Ω_{ex} profile, as shown in Fig. 11. The minima of $\Omega_{ex}(L)$ correspond to N lamellar layers adsorbed in the slit. The adsorbed phases are deformed in the middle of the slit for separations up to $L = 22 = 5\lambda + \lambda/2$, see Fig. 12a, while for larger separations the strain releases to some extent by creating lamellar films with suppressed amplitude, see Fig. 12b. $\Omega_{ex}(L)$ does not approach zero with increasing L. This resembles the behavior of lamellar phases, induced by confinement from microemulsions with short periods ($\lambda/2\pi\xi < \sqrt{3}$) obtained in the GS model [40] and discussed above.

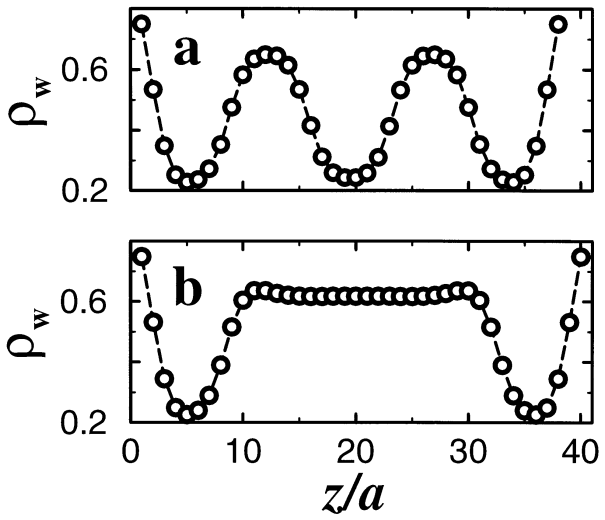

Figure 10. **a**: Density distribution of water between hydrophilic walls for the separation $L = 38$ (the third minimum in Fig. 9a). **b**: Density distribution of water between hydrophilic walls for the separation $L = 40$. For such density distributions the solvation force vanishes. The parameters are the same as in Fig. 9 ($\tau = 0.84$, $\mu = 0.778$, $c/b = 1$, $|\Delta\mu| = 0.001$).

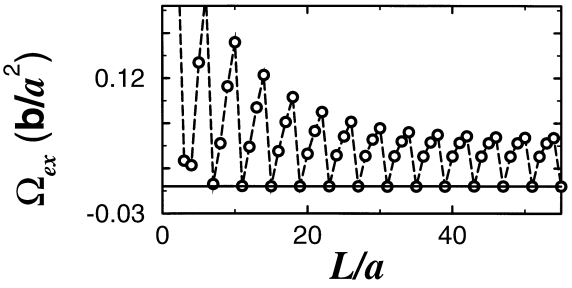

Figure 11. Excess thermodynamic potential Ω_{ex} (in units of b) as a function of the wall separation in the one-dimensional case. The thermodynamic variables τ, μ and the material constant c/b correspond to stability of the shrunk lamellar phase with the period of density oscillations equal to 4 ($\tau = 2.8$, $\mu = 4.32$, $c/b = 4$). Solid line corresponds to vanishing Ω_{ex}.

Comparison with experiments. The compressibility modulus was measured in [22] for system comprised of sodium bis(2-ethylhexyl) sulfosuccinate and brine at $T = 25°C$. For different volume fractions of the surfactant, $\overline{B}$ ranges from 0.003 to 0.027 when expressed in units of k_bT/a^3 (the thickness of the membrane is $a = 1.9$ nm for the system studied in [22]). The results obtained in the CHS model are of the same order of magnitude as in experiments. For the range of parameters chosen in [65], periods of the lamellar phase (in the length unit of a) in the model and in the experimental systems of [22] are comparable. The values of $\overline{B}$ (in units of k_bT/a^3) and κ (in units of k_bT) in the model and experiment agree very well and the agreement is better in the

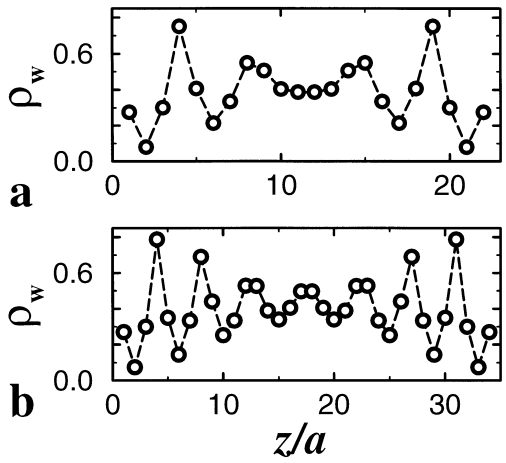

Figure 12. Density profiles of water between water-covered walls for parameters $\tau = 2.8$, $\mu = 4.32$, c/b = 4, **a**: $L = 22$ and **b**: $L = 34$.

three-dimensional model (compare Fig. 6 here and Fig. 8 in [22]). Hence, once the model parameters are chosen, such that the dimensionless period of the bulk lamellar phase is the same as in the experiment, the elastic properties of the confined model and experimental systems agree quantitatively very well. We obtain the same orders of magnitude as in experiments [98] also for lamellar phases induced by confinement. In the case of the shrunk lamellar phases, the discreteness of the model may play an important role. We should note, however, that in experiments of [22] an oscillating solvation force was observed in some cases for all the measured distances, up to $L = 1000a$.

4. SUMMARY

The CHS model is particularly suitable for studying self-assembling systems in restricted geometries. First, the phase transitions between various phases can be continuous or discontinuous in the CHS model already in MF. This allows for relatively easy calculations, close to the coexistence between phases in which self-assembled monolayers are ordered or disordered in space. In particular, such coexisting phases can be studied in the semiinfinite geometry. The model thus can serve for testing of quite general predictions concerning wetting phenomena in such complex systems. Second, swollen lamellar phases incommensurate with the lattice are stable in this model. Periods of such phases are much larger than the lattice constant and change continuously when the thermodynamical conditions are varied. Hence, the lattice structure should only weakly affect the physical properties of the results. At the same time the lattice structure significantly simplifies the calculations. Last but not least, the results can be directly compared with experiments. The interaction parameters can be chosen so that the structure of the bulk phase (in units of the thickness of the

monolayer) is the same as in experimental systems. Then there are no free parameters for fitting to the experimental data. The calculated and measured quantities, such as the elastic moduli, if expressed in terms of k_bT and the thickness of the monolayer (identified with the lattice constant), are in very good quantitative agreement. This finding is encouraging for future applications of the CHS model.

Acknowledgments*

A. Ciach would like to thank Prof. Stell for inspiring collaboration, which has also influenced the present work. It has been a great pleasure and an honour to work with Prof. Stell. This work was partially supported by the Polish State Committee for Scientific Research (grant 3 T09A 073 16).

REFERENCES

1. Tabony J., *Nature*, **319**, 400 (1986).
2. Gozdz W.T. and Hołyst R., *Macromol. Theory Simul*., **5**, 321 (1996).
3. Gozdz W.T. and Hołyst R., *Phys. Rev. E*., **54**, 5012 (1996).
4. Schick M., *Physica A*, **251**, 1 (1998).
5. Scriven L.E., *Nature*, **263**, 123 (1976).
6. Fisher M.E. and Widom B., *J. Chem. Phys*., **50**, 3756 (1969).
7. Stephenson J., *J. Math. Phys*., **11**, 420 (1970).
8. Gompper G. and Schick M., *Self-Assembling Amphiphilic Systems*, volume 16 of *Phase Transitions and Critical Phenomena*, Academic Press, first edition, 1994.
9. Helfrich W., *Z. Naturforsch*., **28 c**, 693 (1973).
10. Nelson D., Piran T. and Weinberg S., editors, *Statistical Mechanics of Membranes and Surfaces*, World Scientific, Singapure, 1989.
11. Gompper G. and Kroll D.M., *Phys. Rev. Lett*., **81**, 2284 (1998).
12. Morse D.C., *Phys. Rev. E*, **50**, R2423 (1994).
13. de Gennes P.G. and Taupin C., *J. Phys. Chem.-US*, **86**, 2294 (1982).
14. Israelachvili J.N. and McGuiggan P.M., *Science*, **241**, 795 (1988).
15. Helfrich W., *Z. Naturforsch*., **33 a**, 305 (1978).
16. Leibler S. and Lipowsky R., *Phys. Rev. B*, 35, 7004 (1987).
17. Lipowsky R. and Leibler S., *Phys. Rev. Lett*., **56**, 2541 (1986).
18. Peliti L. and Leibler S., *Phys. Rev. Lett*., **54**, 1690 (1985).
19. de Gennes P.G., *J. Phys. (Paris)*, Colloque 4, C4 (1969).
20. Harbich W., Servuss R.M. and Helfrich W., *Z. Naturforsch*., **33 a**, 1013 (1978).
21. Skouri M., Marignan J., Appell J. and Porte G., *J. Phys. II France,* **1**, 1121 (1991).
22. Antelmi D.A. and Kékicheff P., *J. Phys. Chem. B*, **101**, 8169 (1997).
23. Paz L., di MeglioJ.M., Dvolaitzky M., Ober R. and Taupin C., *J. Phys. Chem.-US*, **88**, 3415 (1984).
24. Allain M., Oswald P. and di Meglio J.M., *Mol. Cryst. Liq. Crys. B*, **162**, 161 (1988).
25. Gompper G. and Kraus M., *Phys. Rev. E*, **47**, 4289 (1993).
26. Hołyst R. and Gozdz W.T., *J. Chem. Phys*., **106**, 4773 (1997).
27. Hołyst R., *Curr. Opin. Colloid. In*., **3**, 422 (1998).
28. Golubović L., *Phys. Rev. E*, **50**, R2419 (1994).

29. Matsen M.W., Schick M. and Sullivan D.E., *J. Chem. Phys*., **98**, 2341 (1993).
30. Gompper G. and Schick M., *Phys. Rev. Lett*., **65**, 1116 (1990).
31. Lichterfeld F., Schmeling T. and Strey R., *J. Phys. Chem.-US*, **90**, 5762 (1986).
32. Teubner M. and Strey R., *J. Chem. Phys*., **87**, 3195 (1987).
33. Jinnai H., Hashimoto T., Lee D.D. and Chen S.H., *Macromol*., **30**, 130 (1997).
34. Chen S.H., Lee D.D. and Chang S.L.J., *J. Mol. Struct*., **296**, 259 (1993).
35. Gozdz W.T., *Statistical theory of mixtures with surfactants*, Ph.D. Thesis, Institute of Physical Chemistry, Polish Academy of Sciences, Warsaw, 1996.
36. Gelbart W.N., Ben-Shaul A. and Roux D., editors, *Micelles, Membranes, Microemulsions, and Monolayers*, Springer-Verlag, NY, 1994.
37. Gompper G. and Zschocke S., *Europhys. Lett*., **16**, 731 (1991).
38. Gompper G. and Goos J., *Phys. Rev. E*, **50**, 1325 (1994).
39. Gompper G. and Schick M., *Phys. Rev. E*, **49**, 1478 (1994).
40. Schmid F. and Schick M., *Phys. Rev. E*, **48**, 1882 (1993).
41. Lee D.D., Chen S.H., Majkrzak C.F. and Satija S.K., *Phys. Rev. B*, **52**, R29 (1995).
42. Gompper G. and Zschocke S., *Phys. Rev. A*, **46**, 4836 (1992).
43. da Gama M.M.T. and Gubbins K.E., *Mol. Phys*., **59**, 227 (1986).
44. da Gama M.M.T. and Thurtell J.H., *J. Chem. Soc. Farad. Trans. II*, **82**, (1986).
45. da Gama M.M.T., *Mol. Phys*., **63**, 585 (1987).
46. Gunn J.R. and Dawson K.A, *J. Chem. Phys*., **91**, 6393 (1989).
47. Widom B., *J. Chem. Phys*., **84**, 6943 (1986).
48. Ciach A., Høye J.S. and Stell G., *J. Phys. A*, **21**, L777 (1988).
49. Gompper G. and Schick M., *Chem. Phys. Lett*., **163**, 475 (1989).
50. Gompper G. and Schick M., *Phys. Rev. Lett*., **62**, 1647 (1989).
51. Dawson K.A. and Kurtović Z., *J. Chem. Phys*., **92**, 5473 (1990).
52. Matsen M.W. and Sullivan D.E., *Phys. Rev. A*, **41**, 2021 (1990).
53. Laradji M., Guo H., Grant M. and Zuckermann M.J., *Phys. Rev. A*, **44**, 8184 (1991).
54. Gunn J.R. and Dawson K.A., *J. Chem. Phys*., **96**, 3152 (1992).
55. Matsen M.W. and Sullivan D.E., *Phys. Rev. A*, **46**, 1985 (1992).
56. Slotte P.A., *Phys. Rev. A*, **46**, 6469 (1992).
57. Ciach A., Høye J.S. and Stell G., *J. Chem. Phys*., **90**, 1214 (1989).
58. Ciach A. and Poniewierski A., *J. Chem. Phys*., **100**, 8315 (1994).
59. Buzano C., Evangelista L.R. and Pelizzola A., *Phys. Rev. E*, **56**, 770 (1997).
60. Buzano C., Pelizzola A. and Pretti M., *Adv. Phys*., **262**, 280 (1999).
61. Renlie L., Høye J.S., Skaf M.S. and Stell G., *J. Chem. Phys*., **95**, 5305 (1991).
62. Ciach A., *J. Chem. Phys*., **93**, 5322 (1990).
63. Ciach A., Høye J.S. and Stell G., *J. Chem. Phys*., **95**, 5300 (1991).
64. Ciach A., *J. Chem. Phys*., **96**, 1399 (1992).
65. Tasinkevych M. and Ciach A., *Phys. Rev. E*, **60**, 7088 (1999).
66. Tasinkevych M. and Ciach A., *J. Chem. Phys*., **110**, 7548 (1999).
67. Ciach A., *J. Chem. Phys*., **104**, 2376 (1996).
68. de Gennes P.G., *Rev. Mod. Phys*., **57**, 827 (1985).
69. Sullivan D.E. and da Gama M.M.T., in *Fluid Interfacial Phenomena*, C.A. Croxton, ed., Wiley, NY, 1986, (45–135).
70. Dietrich S., *Wetting Phenomena*, volume 12 of *Phase Transitions and Critical Phenomena*, Academic Press, London, first edition, 1988, (1–218).
71. Schick M., in *Liquids and Interfaces*, J. Charvolin, J.F. Joanny and J. Zinn-Justin, eds., Les Houches 1988, Session XLVIII, North Holland, Amsterdam, 1990, (415–497).
72. Diehl H.W., *Field-theoretic Approach to Critical Behavior at Surfaces*, volume 10 of *Phase Transitions and Critical Phenomena*, Academic Press, London, first edition, 1986, (75–267).
73. Evans R., *Adv. Phys*., **28**, 143 (1979).
74. Nakanishi H. and Fisher M.E., *J. Chem. Phys*., **78**, 3279 (1983).
75. Evans R. and Marconi U.M.B., *Chem. Phys. Lett*., **114**, 415 (1985).

76. Tarazona P., Marconi U.M.B. and Evans R., *Mol. Phys*., **64**, 573 (1987).
77. Evans R. and Marconi U.M.B., *J. Chem. Phys*., **86**, 7138 (1987).
78. Ball P.C. and Evans R., *J. Chem. Phys*., **89**, 4412 (1988).
79. Peterson B.K., Gubbins K.E., Heffelfinger G.S., Marconi U.M.B. and van Swol F., *J. Chem. Phys*., **88**, 6487 (1988).
80. Peterson B.K., Heffelfinger G.S., Gubbins K.E. and van Swol F., *J. Chem. Phys*., **93**, 679 (1990).
81. Evans R., *J. Phys.-Condens. Mat*., **2**, 8989 (1990).
82. Ciach A., Tasinkevych M. and Maciołek A., *Europhys. Lett*., **45**, 495 (1999).
83. Lipowsky R., *J. Appl. Phys*., **55 (6)**, 2485 (1984).
84. Zhou X.L., Lee D.D., Chen S.H. and Strey R., *Phys. Rev. A*, **46**, 6479 (1992).
85. Lee D.D. *et al*., *Physica B*, **221**, 296 (1996).
86. Steitz R., Braun C., Lang P., Reiss G. and Findenegg G.H., *Physica B*, **234**, 377 (1997).
87. Derjaguin B.V., Churajev N.V. and Müller V.M., *Surface Forces*, Consultants Bureau, NY, 1987.
88. Israelachvili J.N. and Adams G.E., *J. Chem. Soc. Farad. Trans. 1*, **74**, 975 (1979).
89. Horn R.G. and Israelachvili J.N., *J. Chem. Phys*., **75**, 1400 (1981).
90. Kékicheff P. and Christenson H.K., *Phys. Rev. Lett*., **63**, 2823 (1989).
91. Richetti P., Kékicheff P., Parker J.L. and Ninham B.W., *Nature*, **346**, 252 (1990).
92. Kékicheff P., Richetti P. and Christenson H., *Langmuir*, **7**, 1874 (1991).
93. Roux D. and Safinya C.R., *J. Phys. (Paris)*, **49**, 307 (1988).
94. Nallet F., Roux D. and Prost J., *Phys. Rev. Lett*., **62**, 276 (1989).
95. Roux D., Coulon C. and Cates M.E., *J. Phys. Chem.-US*, **96**, 4174 (1992).
96. Hołyst R. and Oswald P., *Phys. Rev. Lett*., **79**, 1499 (1997).
97. Hołyst R. and Oswald P., *J. Chem. Phys*., **109**, 11051 (1998).
98. Richetti P., Kékicheff P. and Barois P.J., *J. Phys. II France*, **5**, 1129 (1995).